

# Antibacterial Carbon Nanotubes by Impregnation with Copper Nanostructures

HUMBERTO PALZA,<sup>1,3</sup> NATALIA SALDIAS,<sup>1</sup> PAULO ARRIAGADA,<sup>1</sup>  
PATRICIA PALMA,<sup>2</sup> and JORGE SANCHEZ<sup>1</sup>

1.—Departamento de Ingeniería Química y Biotecnología, Facultad de Ciencias Físicas y Matemáticas, Universidad de Chile, Santiago, Chile. 2.—Laboratorio microbiología oral área Péptidos y compuestos antimicrobianos, Facultad de Odontología, Universidad de Chile, Santiago, Chile. 3.—e-mail: hpalza@ing.uchile.cl

The addition of metal-based nanoparticles on carbon nanotubes (CNT) is a relevant method producing multifunctional materials. In this context, CNT were dispersed in an ethanol/water solution containing copper acetate for their impregnation with different copper nanostructures by either a non-thermal or a thermal post-synthesis treatment. Our simple method is based on pure CNT in an air atmosphere without any other reagents. Particles without thermal treatment were present as a well-dispersed layered copper hydroxide acetate nanostructures on CNT, as confirmed by scanning and transmission (TEM) electron microscopies, and showing a characteristic x-ray diffraction peak at 6.6°. On the other hand, by thermal post-synthesis treatment at 300°C, these layered nanostructures became Cu<sub>2</sub>O nanoparticles of around 20 nm supported on CNT, as confirmed by TEM images and x-ray diffraction peaks. These copper nanostructures present on the CNT surface rendered antibacterial behavior to the resulting hybrid materials against both *Staphylococcus aureus* and *Escherichia coli*. These findings present for the first time a simple method for producing antibacterial CNT by direct impregnation of copper nanostructures.

## INTRODUCTION

Copper and its compounds are outstanding materials with a broad range of applications depending on their chemical composition and size. For instance, copper(II) oxide (CuO) is an important semiconductor that is used as a field-emission, high-temperature superconductor, giant magneto-resistance material, and electrode for solar cells.<sup>1,2</sup> Copper(I) oxide (Cu<sub>2</sub>O) is a promising material for both inexpensive photovoltaic power devices and photoelectrochemical cells.<sup>3</sup> Because the chemical and physical properties of copper are strictly dependent on its morphology, considerable efforts have been made in recent years to synthesize various types of nanostructures.<sup>4</sup> A number of different techniques are currently used to control the size and morphology of these nanomaterials.<sup>4</sup> Although most of these reports are focused on copper oxide, controlled synthesis of hierarchical nano-structured copper metal is also possible.<sup>5</sup> These copper

nanoparticles can be used in several applications such as catalysts, photoactive reactions, electrochemical processes, organic electronic devices, and sensors, among others.<sup>6–8</sup> Of all the applications of copper nanoparticles, those related to their strong antimicrobial behavior have increased over the last years, allowing the production of a broad range of novel biocidal materials.<sup>9–14</sup>

An approach for the production of copper nanostructures is by using carbon nanotubes (CNT) as support or template, taking advantage of their outstanding intrinsic properties such as electrical conductivity, chemical interactions, and high specific area.<sup>15</sup> Different methods can be used to synthesize copper/CNT nanostructures, such as dissolution of copper salts in a water/CNT suspension where the solvent is evaporated after stirring at 100°C. The product is reduced by H<sub>2</sub> at temperatures below 573°C, producing copper metal.<sup>16</sup> Laser ablation of Cu in the presence of He gas is another strategy for modifying CNT having oxidized copper

nanoparticles.<sup>17</sup> Another approach is the dispersion of both CNT and copper acetate in ethanol at 75°C until the solvent is evaporated.<sup>18</sup> The particles were then calcined below 500°C, producing copper metal nanoparticles of around 60 nm. Another method was based on a Fehling reaction producing Cu<sub>2</sub>O nanoparticles with sizes around 25 nm supported on CNT.<sup>19</sup> Acid treatment of CNT was also reported for impregnation of Cu<sub>2</sub>O and Cu nanoparticles with sizes of 15–90 nm using nitric acid and xylene solution of copper(I) phenylacetylide at 90°C.<sup>3</sup> A similar treatment was used for electrodeless deposition of a copper metal layer on CNT.<sup>20</sup> Copper acetate dissolved in water with NH<sub>3</sub>-H<sub>2</sub>O and CNT can be further used for the production of CuO, Cu<sub>2</sub>O, and Cu nanoparticles of around 20 nm by a calcination process.<sup>21</sup> Oxygen-functionalized CNT irradiated by infrared has also been used to impregnate CuO, Cu<sub>2</sub>O, and Cu nanoparticles of around 10 nm.<sup>22</sup> More complex processes have been reported recently, producing CNT/metal copper hybrid nanomaterials for sensing and catalyst applications.<sup>23–25</sup>

Despite the potential biocidal behavior of these CNT/copper nanostructures, their antimicrobial properties have been barely assessed.<sup>26</sup> Although either pure or functionalized CNT can present antimicrobial behavior,<sup>27–29</sup> impregnation with copper nanostructures can represent a low-cost and versatile method for the development of antimicrobial CNT. The goal of this work is to present a simple in situ impregnation method for the production of copper nanostructures on CNT. The methodology uses copper acetate dissolved in ethanol/water having dispersed CNT without any other reagents or treatment. The resulting particles were calcined at 300°C. The characterization of the copper compounds produced after impregnation with non-thermal treatment was also considered.

## EXPERIMENTAL

The multiwalled carbon nanotubes (CNT) were supplied by Bayer Material Science (Baytubes C150P) and used without further modification. Copper(II) acetate monohydrate (Cu(CH<sub>3</sub>COO)<sub>2</sub>H<sub>2</sub>O) from May & Baker was used as the main precursor. The dissolution medium was a mixture of 95 wt.% ethanol (C<sub>2</sub>H<sub>6</sub>O) with 5 wt.% water supplied by Winkler.

For the synthesis of the copper structures, 0.9 g of CNT was dispersed in 100 mL of the ethanol/water solution using sonication for 10 min. The dispersion was then mixed with another 100 mL of ethanol/water solution containing 3.8 g of copper acetate at 60°C. The final solution was mixed by sonication during 2 h at 60°C and later filtered and dried for 24 h. The same CNT/copper acetate solution was alternatively mixed at 80°C until the solvent was

evaporated and the product was then dried for 24 h. In both methods, the products were calcined in an oven for 2 h at 300°C at a heating rate of 7°C/min.

X-ray diffraction (XRD) analysis was performed on a Siemens D-5000 diffractometer with a scintillation detector diffraction system and Bragg–Brentano geometry operating with a Cu  $\alpha_1$  radiation source filtered with a graphite monochromator ( $k = 1.5406 \text{ \AA}$ ) at 40 kV and 30 mA in the  $2\theta$  2–80° range at a scanning rate of 0.02°/s. The morphology and elemental analysis of the particles were performed on a field emission scanning electron microscope (FEI-SEM; Inspect 50) coupled with an energy-dispersive x-ray spectroscopy (EDS) equipment. Transmission electron microscopy (TEM) (Tecnai F20 FECS/TEM) operating at 120 kV was further used for high-resolution images.

The antibacterial activity of the synthesized particles was tested against *Escherichia coli* (Gram-negative) and *Staphylococcus aureus* (Gram-positive) bacteria using the Agar Spot Test. A few isolates of *E. coli* and *S. aureus* were inoculated in TSB broth for 18 h at 37°C to get a bacterial suspension in exponential phase which was serially diluted to match a 0.5 McFarland turbidity standard bacterial suspension ( $1 \times 10^8$  colony-forming units (CFU)/mL). A Petri plate was streaked to form a bacterial lawn. Solutions containing 2 wt.% and 4 wt.% of the particles were prepared and dropped (10  $\mu$ L) over the bacterial lawn. Simultaneously, chlorhexidine 0.12 vol.% used as positive control of activity and 0.9% saline buffer as a negative control. All experiments were performed in duplicate. The plates were incubated at 37°C for 20–24 h, depending on the growth of the indicator strain. The appearance of an inhibitory of growth zone larger than 3 mm of diameter was considered as a positive inhibition on the indicator strain. The reported values are the diameter (mm) of the halo when a solution with a certain particle concentration (2 wt.% or 4 wt.%) was added after inoculation of the bacteria.

## RESULTS AND DISCUSSION

Figure 1 shows SEM and TEM images of the particles obtained by the copper impregnation method on CNT with non-thermal treatment. Together with CNT bundles, well-dispersed layered structures appeared without any evidence of micrometric copper salt crystals. These nanostructured layers were a few nanometers thick, around 300 nm wide, and a few nm long. Figure 1d shows semi-transparent layer compounds confirming the small thickness of the particles. The XRD patterns of these particles (Fig. 2) further confirmed the synthesis of a layered morphology, showing a low angle peak at  $2\theta = 6.8^\circ$ . It is noteworthy that the intensity of this peak depended on the method used, with the filtered samples displaying a larger value than the

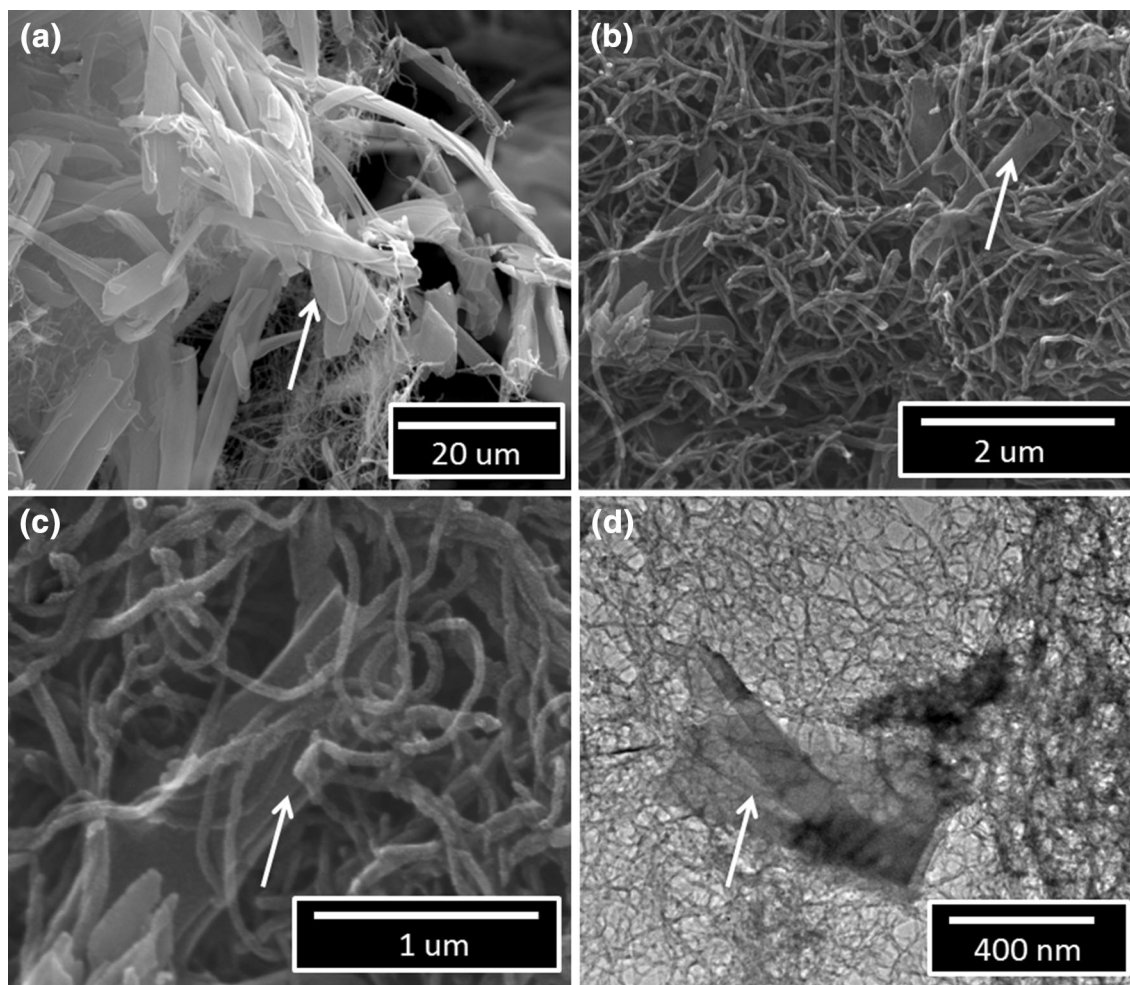


Fig. 1. Electron microscopy images of hybrid CNT/copper particles with non-thermal treatment. (a–c) Scanning electron microscopy images at  $\times 50,000$ ,  $\times 120,000$ , and  $\times 300,000$  magnification, respectively; (d) transmission electron microscopy at  $\times 50,000$  magnification. Arrow indicates the layered structure.

evaporated samples. EDS elemental analysis of these samples showed the presence of carbon (73 at.%) and copper (26 at.%) atoms.

The presence of copper nanostructures with layered morphology can be associated with the formation of specific hydroxides from copper acetate having a botallackite-type structure, such as  $\text{Cu}_2(\text{OH})_3(\text{CH}_3\text{CO}_2)_2\text{H}_2\text{O}$ .<sup>30</sup> In these systems, diffraction peaks at low  $2\theta$  angles are directly related to the basal distance and harmonic reflections, as seen in Fig. 2. In the case of copper hydroxide acetate, this peak appears at  $2\theta = 11^\circ$  with a harmonic at  $2\theta = 22^\circ$ , although either exchange reactions or hydration can shift this pattern to lower  $2\theta$  values due to the increase of the basal distance.<sup>30–32</sup> Layered copper hydroxide acetate can be synthesized by controlled precipitation adding an alkaline solution such as NaOH or by heating a copper acetate water solution in the range of 50–75°C, as in our case.<sup>31,33</sup> To our knowledge, this is the first report synthesizing  $\text{Cu}_2(\text{OH})_3(\text{CH}_3\text{CO}_2)_2\text{H}_2\text{O}$  layer compounds in the presence of CNT.

From Fig. 1b and c it is clear that the presence of hydroxide layer particles between CNT indicates a relevant role in their synthesis. CNT can adsorb molecules via non-covalent forces.<sup>34</sup> In the particular case of copper, CNT are used as a pre-concentration system for adsorption of its ions.<sup>35–38</sup> CNT further interact with the ethanol/water mixture.<sup>39</sup> Therefore, we hypothesize that the local higher concentration of copper ions surrounding CNT drive their precipitation, forming layered  $\text{Cu}_2(\text{OH})_3(\text{CH}_3\text{CO}_2)_2\text{H}_2\text{O}$  despite the low concentration of water.

Figure 2 also displays the XRD patterns of samples after a thermal treatment. The diffraction peaks from both copper acetate and layered hydroxide copper acetate were replaced mainly by copper oxide ( $\text{Cu}_2\text{O}$ ) peaks at  $2\theta = 36.5^\circ$ ,  $42.1^\circ$ ,  $61.4^\circ$ , and  $73.4^\circ$ . This change means that the calcination temperature was enough to produce a decomposition of organic and hydroxide phases.  $\text{Cu}_2(\text{OH})_3(\text{CH}_3\text{CO}_2)_2\text{H}_2\text{O}$  layers present multi-step thermal decomposition associated with: (1) water loss at 120°C; (2) acetate decomposition forming



$\text{Cu}_2\text{O}(\text{OH})_2$  at  $180^\circ\text{C}$ ; and (3) oxidation forming  $\text{Cu}_2\text{O}$  at  $220^\circ\text{C}$ .<sup>33</sup> Copper acetate otherwise presented a characteristic two-step process associated with dehydration between  $100^\circ\text{C}$  and  $190^\circ\text{C}$  and decomposition of copper acetate between  $220^\circ\text{C}$  and  $320^\circ\text{C}$ .<sup>40</sup> SEM images of these calcined particles are displayed in Fig. 3, showing that on the CNT surface sub-micrometric particles were homogeneously formed (Fig. 3a and b). Indeed, TEM images of these calcined particles, displayed in Fig. 3c, led to the conclusion that mainly nanoparticles of around 20 nm were produced. Therefore, thermal decomposition of our hybrid CNT/copper-layered materials produced copper oxide nanoparticles at just  $300^\circ\text{C}$ . This is further confirmed by EDS elemental analysis during SEM observations,

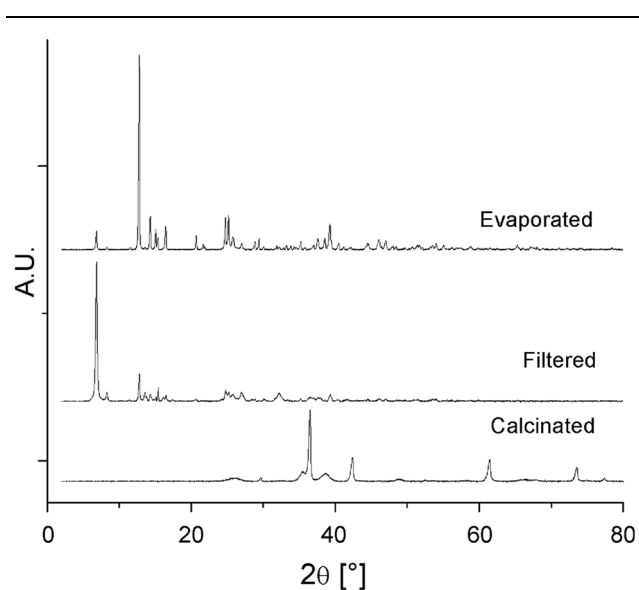


Fig. 2. X-ray diffraction patterns from the different samples prepared. Samples with non-thermal treatment filtered and evaporated, and samples with thermal treatment.

showing that these hybrid particles mostly presented carbon (78 at.%), oxygen (19 at.%), and copper (3 at.%) atoms.

Table I shows the results of the antibacterial activity of the different hybrid samples, including pure CNT. Without copper impregnation, CNT did not inhibit bacterial growth. On the other hand, CNT/copper hybrid nanoparticles created a halo, with a statistical significance as compared with pure CNT, on the agar plate associated with a zone where bacteria were unable to grow, meaning that both copper nanoparticles rendered antibacterial behavior to CNT. It should be noted that the sizes of the halos were similar to those obtained using chlorhexidine at the same dilution, showing the high antibacterial performance of the hybrid CNT/copper particles.<sup>41</sup> Moreover, no statistical differences were found between the hybrid particles, and chlorhexidine. To our knowledge, this is not only the first report about the antibacterial activity of CNT/copper hybrid materials produced by in situ synthesis but also about the biocidal behavior of layered copper hydroxide acetate.

At 2 w/w%, CNT with copper oxide particles were not active against *E. coli*, while CNT/layered copper at the same concentration displayed an inhibiting behavior having statistical significance. However, this oxide copper material was active against *S. aureus* at 2 w/w%, meaning that greater effect of hybrid particles on Gram-positive than on Gram-negative bacteria, especially at low concentrations. The latter is a general tendency also found with other copper-based antimicrobial materials, for instance in polymer composites.<sup>42,43</sup> The mechanism of the toxicity of copper to microorganisms can be explained by several processes such as the displacement of essential metals from their native binding sites or through ligand interactions.<sup>44</sup> Copper(II) ions are able to form organic complexes with biomolecules having sulfur-, nitrogen- or oxygen-bearing groups present in the microorganisms. This may either cause defects in the conformational structure of nucleic acids and proteins or changes

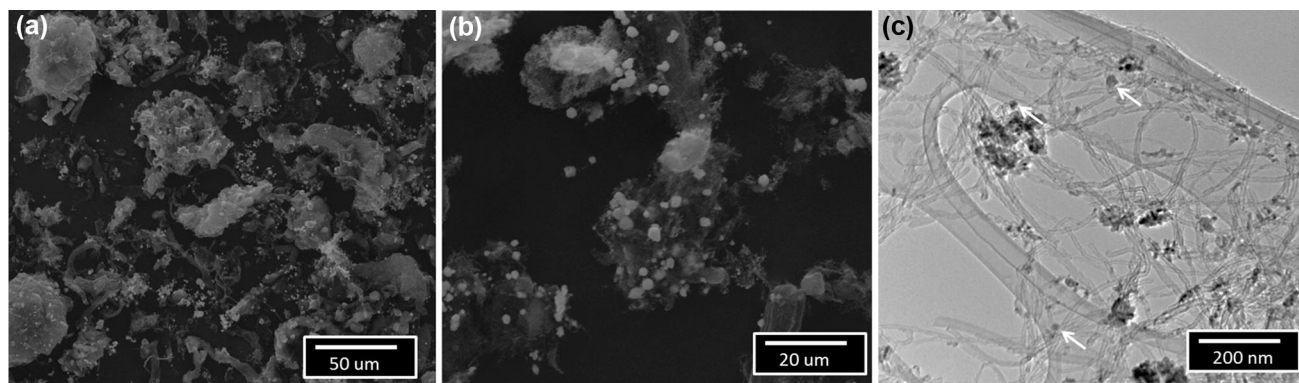


Fig. 3. Electron microscopy images of copper/CNT hybrid particles with thermal treatment. (a, b) Scanning electron microscopy images at  $\times 1000$  and  $\times 4000$  magnification, and (c) transmission electron microscopy at  $\times 100,000$  magnification. Examples of isolated particles of around 20 nm are indicated by arrows.

**Table 1. Antimicrobial results from the synthesized particles: CNT with layered copper hydroxide acetate (CNT + LCA) and CNT with particles after calcination (CNT + CC) (See “Experimental” section for details)**

Sample	<i>E. coli</i>		<i>S. aureus</i>	
	2%	4%	2%	4%
CNT	–	–	–	–
CNT + LCA	8	9	14	16
CNT + CC	–	9	10	12
CHX	18	19	16	18

in oxidative phosphorylation reactions and in osmotic balance. Membrane damage is also a key event explaining the strong antibacterial behavior of copper-based materials.<sup>45</sup>

### CONCLUSION

CNT impregnated with copper nanostructures were produced by a simple method based on an ethanol/water solution containing copper acetate using pure CNT in an air atmosphere and without any further reagents. The hybrid particles with non-thermal post-synthesis treatment presented layered copper hydroxide acetate structures well dispersed through the CNT. In addition, by thermal treatment at 300°C these layered structures became copper oxide particles of around 20 nm in size. It should be noted that both layered copper hydroxide and copper oxide nanoparticles were able to provide an antibacterial behavior to CNT against *S. aureus* and *E. coli*. Our findings present for the first time a simple route which allows the production of novel multifunctional CNT by direct impregnation of copper nanostructures.

### ACKNOWLEDGEMENT

The authors gratefully acknowledge the financial support of CONICYT under FONDECYT Project 1150130.

### REFERENCES

1. Y. Yu and J. Zhang, *Mater. Lett.* 63, 1840 (2009).
2. Z. Zhang, H. Chen, H. Che, Y. Wang, and F. Su, *Mater. Chem. Phys.* 138, 593 (2013).
3. A. Martinez-Ruiz and G. Alonso-Nuñez, *Mater. Res. Bull.* 43, 1492 (2008).
4. F. Bayansal, H.A. Cetinkara, S. Kahraman, H.M. Cakmak, and H.S. Guder, *Ceram. Int.* 38, 1859 (2012).
5. H. Dong, Y. Wang, F. Tao, L. Wang, *J. Nanomaterials*. ID 901842 (2012).
6. M.B. Gawande, A. Goswami, F.X. Felpin, T. Asefa, X. Huang, R. Silva, X. Zou, R. Zboril, and R.S. Varma, *Chem. Rev.* 116, 3722 (2016).
7. A.A. Ensafi, N. Zandi-Atashbar, M. Ghiaci, M. Taghizadeh, and B. Rezaei, *Mater. Scien. Eng. C* 47, 290 (2015).
8. G. Polino, R. Abbel, S. Shanmugam, G.J.P. Bex, R. Hendriks, F. Brunetti, A. Di Carlo, R. Andriessen, and Y. Galagan, *Org. Electron.* 34, 130 (2016).
9. T. Kruk, K. Szczepanowicz, J. Stefańska, R.P. Socha, and P. Warszyńska, *Colloids Surf. B* 128, 17 (2015).
10. C. Gunawan, W.Y. Teoh, C.P. Marquis, and R. Amal, *ACS Nano* 5, 7214 (2011).
11. J.P. Ruparelia, A. Chatterjee, S.P. Duttagupta, and S. Mukherji, *Acta Biomater.* 4, 707 (2008).
12. Z. Wang, N. Li, J. Zhao, J.C. White, P. Qu, and B. Xing, *Chem. Res. Toxicol.* 25, 1512 (2012).
13. N. Cioffi, L. Torsi, N. Ditarantano, G. Tantalillo, L. Ghibelli, L. Sabbatini, T. Bleve-Zacheo, M. D'Alessio, P.G. Zambonin, and E. Traversa, *Chem. Mater.* 17, 5255 (2005).
14. H. Palza, S. Gutiérrez, K. Delgado, O. Salazar, V. Fuenzalida, J. Avila, G. Figueroa, and R. Quijada, *Macromol. Rapid Commun.* 31, 563 (2010).
15. G.G. Wildgoose, C.E. Banks, and R.G. Compton, *Small* 2, 182 (2006).
16. P. Chen, X. Wu, J. Lin, and K.L. Tan, *J. Phys. Chem. B* 103, 4559 (1999).
17. A. Koshio, M. Shiraishi, Y. Kobayashi, M. Ishihara, Y. Koga, S. Bandow, S. Iijima, and F. Kokai, *Chem. Phys. Lett.* 396, 410 (2004).
18. P. Wang, B. Huang, J. Wei, X. Qin, S. Yao, and Q. Zhang, *Mater. Lett.* 61, 5255 (2007).
19. K.R. Reddy, B.C. Sin, C.H. Yoo, W. Park, K.S. Ryu, J.S. Lee, D. Sohn, and Y. Lee, *Scr. Mater.* 58, 1010 (2008).
20. W.M. Daoush, B.K. Lim, C.B. Mo, D.H. Nam, and C.H. Hong, *Mater. Sci. Eng. A* 513–514, 247 (2009).
21. X. Wang, F. Zhang, B. Xia, X. Zhu, J. Chen, S. Qiu, P. Zhang, and J. Li, *Solid State Sci.* 11, 655 (2009).
22. P. Martis, B.R. Venugopal, J.F. Seffer, J. Delhalle, and Z. Mekhalif, *Acta Mater.* 59, 5040 (2011).
23. Y. Fu, L. Zhang, and G. Chen, *Carbon* 50, 2563 (2012).
24. Z. Zhang, Z. Lin, C. Li, and Y. Li, *Mater. Technol.* 30, A186 (2016).
25. G. Kour, M. Gupta, B. Vishwanathan, and K. Thirunavukkarasu, *New J. Chem.* 40, 8535 (2016).
26. L. Sheng, S. Huang, M. Sui, L. Zhang, L. She, and Y. Chen, *Environ. Sci. Eng.* 9, 625 (2015).
27. S. Kang, M. Pinault, L.D. Pfefferle, and M. Elimelech, *Langmuir* 23, 8670 (2007).
28. X. Qi, G. Poernomo, K. Wang, Y. Chen, M.B. Chan-Park, R. Xua, M. Wook, and M. Chang, *Nanoscale* 3, 1874 (2011).
29. A. Amiria, H.Z. Zardini, M. Shanbedi, M. Maghrebi, M. Baniadam, and B. Tolueinia, *Mater. Lett.* 72, 153 (2012).
30. G.G. Carbajal, K.G. Satyanarayana, and F. Wypych, *Solid State Ion.* 178, 1143 (2007).
31. R. Marangoni, G.A. Bubniak, M.P. Cantao, M. Abbate, W.H. Schreiner, and F. Wypych, *J. Colloid Interface Sci.* 240, 245 (2001).
32. V. Prevot, C. Forano, and J.P. Besse, *Appl. Clay Sci.* 18, 3 (2001).
33. N. Masciocchi, E. Corradi, A. Sironi, G. Moretti, G. Minelli, and P. Porta, *J. Solid State Chem.* 131, 252 (1997).
34. K. Pyrzynska, *Anal. Sci.* 23, 631 (2007).
35. M. Tuzen, K.O. Saygi, and M. Soylak, *J. Hazard. Mat.* 152, 632 (2008).
36. P. Liang, Y. Liu, and L. Guo, *Spectrochim. Acta B* 60, 125 (2005).
37. M. Tuzen, K.O. Saygi, and M. Soylak, *J. Hazard. Mater.* 152, 632 (2008).
38. A. Duran, M. Tuzen, and M. Soylak, *J. Hazard. Mater.* 169, 466 (2009).

39. L. Lu, Q. Shao, L. Huang, and X. Lu, *Fluid Phase Equilib.* 261, 191 (2007).
40. V. Bellini, R. Machado, M.R. Morelli, and R.H. Kiminami, *Mater. Res.* 5, 453 (2002).
41. E. Verraedt, M. Pendela, E. Adams, J. Hoogmartens, and J.A. Martens, *J. Control. Release* 142, 47 (2010).
42. H. Palza, R. Quijada, and K. Delgado, *J. Bioact. Compat. Polym.* 30, 366 (2015).
43. A. Muñoz-Bonilla, M.L. Cerrada, and M. Fernández-García, eds., *Polymeric Materials with Antimicrobial Activity* (Spain: Madrid, 2013).
44. G. Borkow and J. Gabbay, *Curr. Med. Chem.* 12, 2163 (2005).
45. A.M. Studer, L.K. Limbach, L. Van Duc, F. Krumeich, E.K. Athanassiou, L.C. Gerbera, H. Moch, and W.J. Stark, *Toxicol. Lett.* 197, 169 (2010).